Hyperfine Interactions (2020) 241: 14
https://doi.org/10.1007/s10751-019-1684-6

Reuse of Fe-based amorphous alloys containing CRM: study on their temperature behavior

Z. Cherkezova-Zheleva[1] · D. Paneva[1] · V. Petkova[2,3] · J. Krstić[4] · G. Stefanov[5]

Published online: 19 December 2019

Abstract
In this paper, the physico chemical properties of Fe–based amorphous alloys containing critical raw materials (CRM) were investigated in order to reuse them for photocatalytic degradation of azo dyes. The iron-based metallic glasses were prepared by melt spinning method. Their chemical composition is: $Fe_{67}B_{14}Co_{18}Si$, $Fe_{78}B_{15}Mo_2Si_5$ and $Fe_{40}B_{16}Ni_{40}Mo_4$. Characterization of the ribbons was done using combination of analytical methods. Studied materials were heated in inert atmosphere and in air at temperature of 1000 °C. Crystallization processes of investigated Fe–based amorphous alloys depending on their chemical composition were registered using thermal analysis. The changes of material phase composition and crystallinity degree were studied using powder X-ray diffraction (XRD) and Mössbauer spectroscopy (MS). The thermal treatment in inert atmosphere above the crystallization temperature of studied amorphous alloys result in rearrangement of iron neighbours and formation of multiphase crystalline structure, which strongly depends on the additive elements (Co, Ni, Mo). Heating of ribbons in air affects significantly the kinetic of crystallization and registered products in comparison to annealing in inert (argon) atmosphere. Investigation of thermal stability of ribbon metallic glasses and formation of different intermediate and product compounds is very important for practical application of damaged amorphous alloys, their further reuse and recycling.

Keywords Fe-based amorphous alloys · Critical raw materials (CRM) · Crystallization · ^{57}Fe Mössbauer spectroscopy · XRD · Thermal analysis

This article is part of the Topical Collection on *Proceedings of the 5th Mediterranean Conference on the Applications of the Mössbauer Effect (MECAME 2019) and 41st Workshop of the French-speaking Group of Mössbauer Spectroscopy (GFSM 2019), Montpellier, France, 19-23 May 2019*
Edited by Pierre-Emmanuel Lippens, Yann Garcia, Moulay-Tahar Sougrati and Mira Ristic (†)

✉ Z. Cherkezova-Zheleva
zzhel@ic.bas.bg

Extended author information available on the last page of the article

1 Introduction

The continuous research interest to the metallic glasses is based on their unique properties, their advantages and potential applications in various fields of techniques and engineering [1–3]. Some key features of the glassy state in metals lead to advances and new opportunities for microstructural design, opening up a broad application of attractive materials. Amorphous alloys could be divided into two categories: metal-metalloid systems such as Fe-B, Co-P, Pd-Si, etc. and metallic systems such as Fe-Zr, Cu-Ti, Ni-Zr, Cu-Zr, etc. The metal-metalloid glasses are very attractive due to their great potential for technical applications. The metallic glasses are very suitable for studying of the fundamental properties of glassy metals. The wide range of solid state compositions, make it possible to study systematic changes of properties as a function of alloy chemical composition. Different elements such as transition metals (TM), rare earth elements (RE), platinum group metals (PGM) have been used in order to improve and stabilize advanced properties of amorphous metallic alloys [1–3]. Some of these elements are included into a list of so-called critical raw materials [4–6]. This list has been created in 2011 by the European Commission and it is subject to a regular review and update every three years. The CRM list for the EU includes raw materials which are crucial to Europe's economy, because they form a strong industrial base for production of a broad range of goods and applications used in everyday life and in modern technologies. On the other hand there is a growing concern within the EU and across the world for the reliable and unhindered access of certain raw materials. CRMs combine raw materials of high importance to the EU economy and of high risk associated with their supply. Sustainable solutions of CRM problem include substitution of CRMs with non-critical materials without lose of technological properties of materials and transition from linear to circular economy, including material reuse and recycling [4–6].

Fe-based bulk metallic glasses are materials at the cutting edge of metal research as they have improved magnetic, electrochemical, tribological and mechanical properties [1–3, 7–14]. The methods for their production are based on rapid solidification from the melt, which gives rise to production of extremely homogeneous materials [1–3]. Amorphous Fe-based alloys are produced in the form of thin ribbons, which is appropriate for application in electronics and electrotechnics for manufacturing of magnetic cores for power supply and small sized high-frequency transformers, magnetic heads, magnetic shields, etc. [7, 8]. However, in some cases these high technological

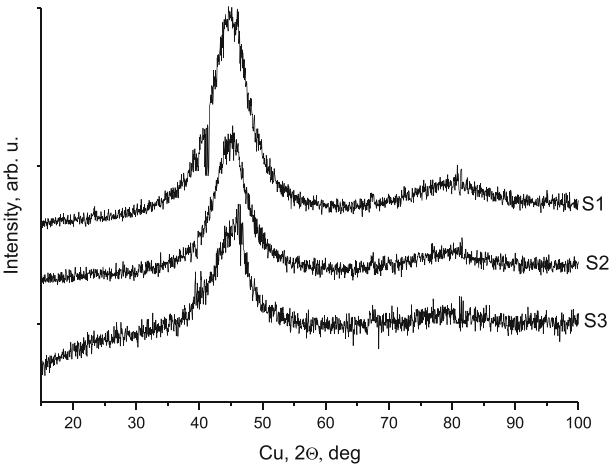

Fig. 1 X-ray diffraction patterns of initial materials: S1 - $Fe_{67}B_{14}Co_{18}Si$; S2 - $Fe_{40}B_{16}Ni_{40}Mo_4$ and S3 - $Fe_{78}B_{15}Mo_2Si_5$

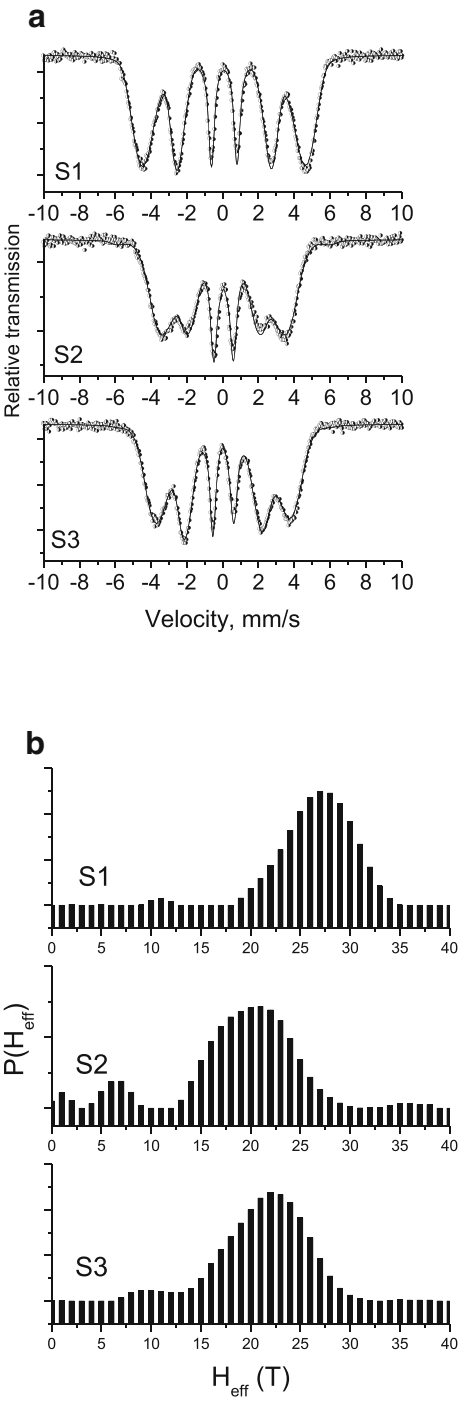

Fig. 2 **a** Room temperature Mössbauer spectra of initial materials: S1 - $Fe_{67}B_{14}Co_{18}Si$; S2 - $Fe_{40}B_{16}Ni_{40}Mo_4$ and S3 - $Fe_{78}B_{15}Mo_2Si_5$; **b** the histograms describing the distribution of hyperfine fields

materials have been damaged due to technological problems during their preparation, inappropriate storage and after their usage. So, the amorphous alloys partially lose some advanced properties. In

Table 1 Mean Mössbauer hyperfine parameters of RT spectra components of the initial ribbons: <IS> – the average isomer shift value given relative to metallic iron at room temperature; <2ε> – the average quadrupolar shift value; <H_{eff}> – the average hyperfine field value; A23 – the relative areas of lines 1/6, 2/5 respect to lines 3/4

Sample	<IS>, mm/s	<2ε>, mm/s	<H_{eff}>, T	A23
$Fe_{67}B_{14}Co_{18}Si$ (S1) - initial	0.08	−0.01	27.6	2.01
$Fe_{40}B_{16}Ni_{40}Mo_4$ (S2) - initial	0.05	−0.01	19.9	1.82
$Fe_{78}B_{15}Mo_2Si_5$ (S3) - initial	0.02	−0.01	22.2	2.02

this regard it is very important to reuse such partially crystallized metallic glasses either after their end-of-life (spent materials) or after their partial damage [5, 6].

The investigation of structural relaxation of amorphous materials has been an object of large number of studies and the basic regularities are already established [1–3, 7–9]. However, a number of not well clarified questions in regard to relaxation processes are still open. Structural changes caused by the relaxation processes directly reflect physical and application properties of amorphous metallic alloys. The aim of this study was to investigate the thermal stability of Fe-based ternary metal-metal-metalloid (Fe-TM-B-Si, TM = Co, Mo) and quaternary (Fe-Ni-Mo-B) glassy alloys as a first step of investigation of their reuse.

2 Experimental

2.1 Materials

Series of Fe-based ternary metal-metal-metalloid (Fe-TM-B-Si, TM = Co, Mo) and quaternary (Fe-Ni-Mo-B) glassy alloys were obtained by melt spinning method. Their chemical composition is: Sample 1 (S1) - $Fe_{67}B_{14}Co_{18}Si$, Sample 2 (S2) - $Fe_{40}B_{16}Ni_{40}Mo_4$ and Sample 3 (S3) - $Fe_{78}B_{15}Mo_2Si_5$.

2.2 Characterization methods

Powder X-ray diffraction patterns were collected within the range of 5.3 to 80° 2θ with a constant step 0.02° 2θ on Empyrean diffractometer with Cu Kα radiation. Phase identification was performed with the X'Pert using ICDD-PDF2 Database.

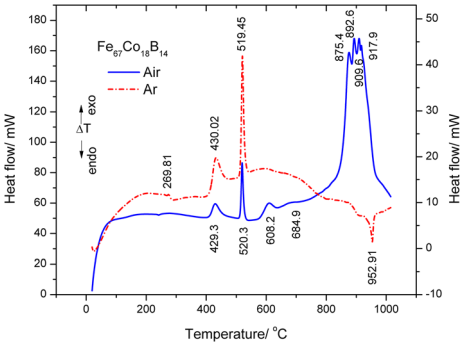

Fig. 3 DSC curves measured for $Fe_{67}B_{14}Co_{18}Si$ in the temperature range from RT to 1000 °C in different gas atmosphere – Ar and air

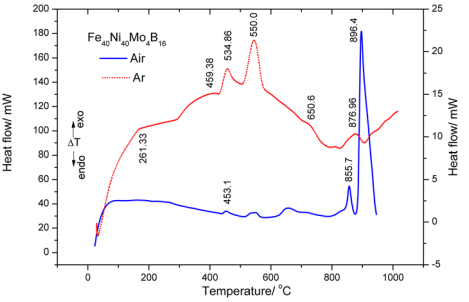

Fig. 4 DSC curves measured for $Fe_{40}B_{16}Ni_{40}Mo_4$ in the temperature range from RT to 1000 °C in different gas atmosphere – Ar and air

Transmission Mössbauer spectra were recorded by Wissenschaftliche Elektronik GmbH electromechanical spectrometer (Germany) at room temperature (RT) and at a constant acceleration mode. The γ-beam produced of ^{57}Co/Rh source (100 mCi) was oriented perpendicular to the ribbon plane. The velocity was calibrated by foil standard and the isomer shift is quoted to that of α-Fe at 300 K. The parameters of hyperfine interactions of the obtained spectral components: isomer shift (IS), quadruple shift (2ε) /quadruple splitting (QS), hyperfine effective field (H_{eff}), line width (FWHM) and partial area of the spectra (A) were determined by WinNormos program. The errors for IS, 2ε, QS, and FWHM are ±0.01 mm/s. The error for H_{eff} is ±0.1 T. The computer fitting was based on the least squares method.

The thermal properties of the samples were investigated using differential scanning calorimetry (DSC). The measurements were performed on a SETSYS2400 thermal analyzer (SETARAM Instr., France) equipped with a DSC-1500 °C heating system (S-type sensor with plate rode) in the temperature range RT – 1200°C, with a heating rate of 10 °C.min^{-1}, sample masse – 18 ± 2 mg, in static air and inert gas – Ar, flow-rate 50 ml.min^{-1}.

3 Results and discussion

The diffractograms of initial materials are shown in Fig. 1. All initial samples used in this study are X-ray amorphous. Their patterns consist of broad halo peaks without indication of any crystallite phases.

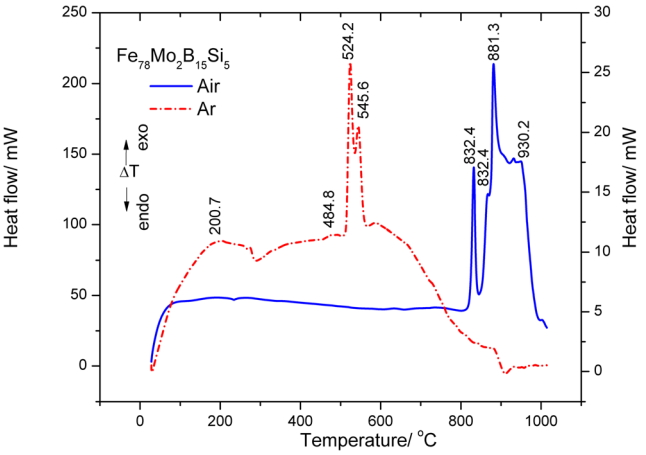

Fig. 5 DSC curves measured for $Fe_{78}B_{15}Mo_2Si_5$ in the temperature range from RT to 1000 °C in different gas atmosphere – Ar and air

Table 2 Data of thermal behaviour of studied ribbons

Sample	Thermal data/ °C		Interpretation
	Air	Ar	
$Fe_{67}B_{14}Co_{18}Si$ (S1)	429.3	430.0	I stage of low temperature crystallization
	520.3	519.5	
	608.2	608.2	
	875.4	–	II stage of high temperature crystallization
	892.6		
	909.6		
	917.9		
$Fe_{40}B_{16}Ni_{40}Mo_4$ (S2)	453.1	459.4	I stage of low temperature crystallization
		534.8	
		550.0	
	855.7	877.0	II stage of high temperature crystallization
	896.4		
$Fe_{78}B_{15}Mo_2Si_5$ (S3)	522.2	524.2	I stage of low temperature crystallization
	543.3	545.6	
	832.4	–	II stage of high temperature crystallization
	868.2		
	881.3		
	930.2		

Room temperature Mössbauer spectra of the initial samples are presented in Fig. 2a. Mössbauer spectrometry is a suitable technique for investigation of the structural and the magnetic properties of amorphous alloy ribbons. Registered spectra are typical for amorphous ferromagnetic metallic glasses and display magnetically split patterns with six broad absorption lines [2, 3]. They can be considered as superpositions of a variety of spectra belonging to iron atoms having different neighbourhood atoms [7–16]. It can be clearly seen (Fig. 2a) that for all registered spectra the line width increases from the inner to the outer lines, which can be related to the existence of a distribution of local hyperfine fields [9]. On the other hand the pattern of the spectra reveals the existence of line asymmetry at negative and positive velocities. Therefore, a distribution in hyperfine parameters was assumed, namely in the magnetic hyperfine field, isomer shift, and quadrupole splitting. The average hyperfine parameters of spectra were determined by least-squares fitting of lines (Table 1). The distributions of hyperfine fields, $P(H_{eff})$ are shown in Fig. 2b. They were obtained by a smooth-histogram processing in the range of $H_{eff} = 0–40$ T. The average isomer shift and the average electric field gradient were obtained close to zero which was considered also for other disordered Fe–Me alloys [7–16]. The area ratio of the lines 1/6, 2/5 in respect to lines 3/4, is varied and the resulting values are displayed in Table 1. The analysis revealed the difference between the shape, maxima and a low-field tail of $P(H_{eff})$. The differences in hyperfine parameters can be regarded to the impact of chemical composition of studied ribbons.

Differential Scanning Calorimetry (DSC) was used for investigation of thermal stability and crystallisation processes of studied amorphous ribbons in two different media – inert atmosphere (Ar gas) and air flow (see Figs. 3, 4 and 5). DSC curves registered for the amorphous alloys revealed broad exothermic peak at low temperatures, which reflects the slow precipitation reactions typical of diffusion controlled primary crystallization [3, 7, 8, 10, 16]. This process is followed by two-stage crystallisation, which could be separated to two temperature regions [10]. The first one is in the interval 420-610°C and the second one is in 850-920°C (see

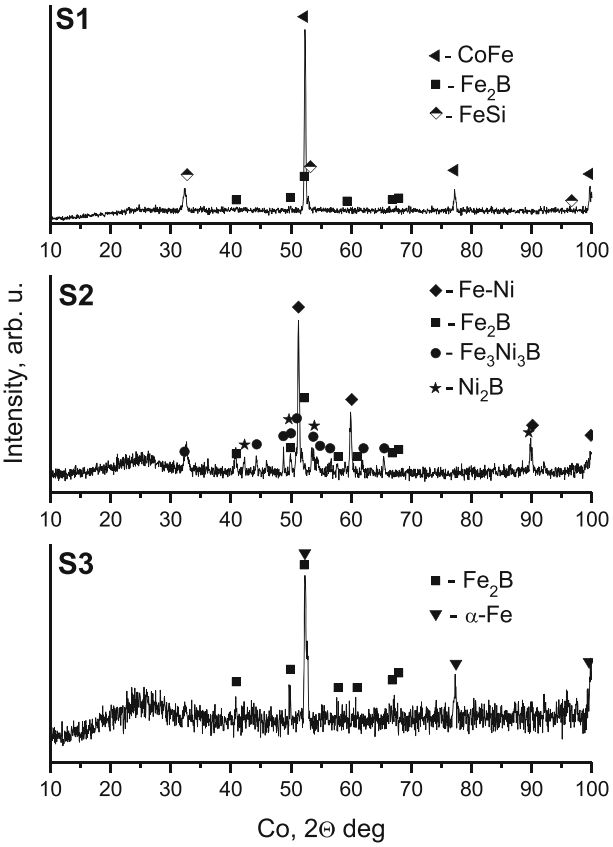

Fig. 6 XRD patterns of thermally treated materials in inert (Ar) atmosphere: S1 - $Fe_{67}B_{14}Co_{18}Si$; S2 - $Fe_{40}B_{16}Ni_{40}Mo_4$ and S3 - $Fe_{78}B_{15}Mo_2Si_5$

Table 2). Both of them are corresponding to exothermal effects. The impact of oxidative (air) atmosphere could be regarded to more intensive crystallization oxidation processes in the samples. The DSC analysis and the data in Table 2 show that no thermal effects were registered in high temperature region of DSC curves of samples $Fe_{67}B_{14}Co_{18}Si$ and $Fe_{78}B_{15}Mo_2Si_5$. This could be regarded to lack of oxidation reactions in this region. Presented temperature maxima obtained by the thermal analysis in the two processing media could be related to different phase transitions and respectively different final phases obtained [7–16].

Phisico-chemical characterisation of thermally treated samples in different atmosphere (Ar and air) was done in order to analyse the stability of studied materials, the results of crystallization reactions and the appearance of new phases. In this regard X-ray diffraction patterns and Mössbauer spectra were very informative to determine the phase composition of the samples and the change of their crystallinity degree after the multi-stage crystallization processes registered by DSC analysis. Combined data obtained using both methods allow the identification of the presented phases. X-ray diffractograms of thermally treated ribbons in inert atmosphere are shown in Fig. 6. They reveal different crystallinity degree of heated materials. Samples $Fe_{40}B_{16}Ni_{40}Mo_4$ (S2) and $Fe_{78}B_{15}Mo_2Si_5$ (S3) partially preserve their amorphous structure, while the ribbon $Fe_{67}B_{14}Co_{18}Si$ (S1) crystallises after thermal treatment in Ar. The pattern analysis identified the formation of metal phase (α-Fe, Fe-Co or Fe-Ni,

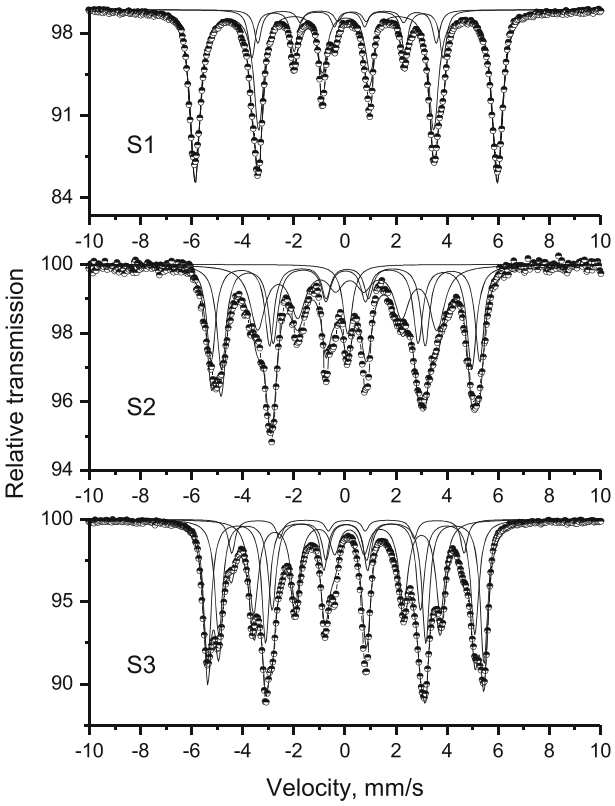

Fig. 7 Mössbauer spectra of thermally treated materials in inert (Ar) atmosphere: S1 - $Fe_{67}B_{14}Co_{18}Si$; S2 - $Fe_{40}B_{16}Ni_{40}Mo_4$ and S3 - $Fe_{78}B_{15}Mo_2Si_5$

respectively) and Fe_2B in all studied cases as a result of thermal treatment in inert atmosphere. Parallel to this FeSi is presented in $Fe_{67}B_{14}Co_{18}Si$ (S1) sample and different compounds were obtained in case of Fe-Ni-Mo (S2) sample: Ni_2B, Fe_3Ni_3B.

Additional information about the redistribution of the elements in the investigated alloys may be obtained from the Mössbauer data. Fitting procedure spectra of thermally treated materials was done by discrete components spectra evaluation due to appearance of crystal phases registered by XRD. The spectra of samples heated in Ar consist of 3 or 4 sextet components (see Fig. 7). According to the obtained Mössbauer spectra these components can be referred to change from amorphous to crystalline state associated with the rearrangements of metallic iron and non-metallic elements included in the matrix [7, 8, 10, 11]. The identified iron-containing phases are given in Table 3 [7]. α- intermetallic phase (BCC structure) and Fe_xB phase are presented in all materials (Fe_2B, Fe_3B and/or FeB) [17]. In addition α-Fe(Si) was registered in Fe-Mo (S3) ribbon. Formation of γ-Fe-Ni alloy was also obtained in Fe-Ni-Mo (S2) sample. The registered changes can be related to the redistribution of elements during the crystallization processes [7, 8].

In order to collect more information about the temperature behaviour of studied ribbons the changes in their composition after heating in air were also registered. The DSC study in air flow (Figs. 3, 4 and 5 and Table 2) shows the genesis and evolution of crystallite phases.

Table 3 Mössbauer hyperfine parameters of RT spectra components of the samples annealed in different atmospheres (inert - Ar and air)

Sample	Components	IS, mm/s	2ε/QS, mm/s	H_{eff}, T	FWHM, mm/s	G, %
$Fe_{67}B_{14}Co_{18}Si$ (S1) - annealed in Ar	Sx1-Fe-Co alloys	0.05	0.00	36.8	0.45	76
	Sx2 –Fe_2B	0.14	0.04	23.8	0.32	15
	Sx3- FeB	0.18	0.09	21.7	0.34	9
$Fe_{67}B_{14}Co_{18}Si$ (S1) - annealed in air	Sx1-α-Fe_2O_3	0.36	−0.20	51.7	0.30	47
	Sx2-γ-Fe_2O_3	0.33	0.00	49.8	0.60	33
	Db1-Fe^{3+} – SPM	0.36	0.63	-	0.37	6
	Db2- Fe^{3+} – SPM	0.39	0.94	-	0.38	14
$Fe_{40}B_{16}Ni_{40}Mo_4$ (S2) - annealed in Ar	Sx1- α-Fe	0.06	0.04	32.7	0.42	30
	Sx2-α-Fe(Mo, Ni)	0.05	0.02	30.9	0.44	33
	Sx3-FeB	0.14	0.05	21.8	0.71	32
	Sn-γ-FeNi	0.03	-	-	0.44	5
$Fe_{40}B_{16}Ni_{40}Mo_4$ (S2) - annealed in air	Sx-α-Fe_2O_3	0.36	−0.20	51.7	0.29	78
	Db-Fe^{3+} – SPM	0.37	0.82	-	0.53	22
$Fe_{78}B_{15}Mo_2Si_5$ (S3) - annealed in Ar	Sx1 – α-Fe	0.03	0.00	33.7	0.35	36
	Sx2-α-Fe(Si)	0.06	0.01	31.2	0.38	29
	Sx3-Fe_3B	0.09	0.02	28.3	0.32	6
	Sx4-Fe_2B	0.13	0.05	23.7	0.34	29
$Fe_{78}B_{15}Mo_2Si_5$ (S3) - annealed in air	Sx1-α-Fe_2O_3	0.36	−0.20	51.7	0.30	78
	Sx2-Fe^{3+}_{tetra} in $Fe_{3-x}O_3$	0.29	0.00	49.1	0.46	9
	Sx3- $Fe^{2.5+}_{octa}$in $Fe_{3-x}O_3$	0.65	0.00	46.2	0.43	7
	Db-Fe^{3+}-SPM	0.37	0.47	-	0.50	7

Sn - singlet; Db - quadrupole doublet; Sx - sextet component; SPM – superparamagnetic phase

Formation of iron oxides (hematite and magnetite) and boron oxides was confirmed by XRD and Mössbauer spectroscopy.

Mössbauer spectra of samples measured after heating of ribbons in air media (Fig. 8) reveal completely different crystallisation behaviour of the ribbons. The spectra can be satisfactorily fitted with set of six-line patterns and doublet components. The results of the least-square fit are listed in Table 3. The hyperfine parameters are characteristic of iron oxide phases – hematite and superparamagnetic (SPM) oxide phase with a collapsed hyperfine magnetic field [17–19]. The relative amount of SPM component is three times higher in S1 and S2 than in S3 ribbon, which is indicative for slower crystallisation process in case of S3 alloy. In addition Fe^{2+} ions were registered in heated S3 sample, but only Fe^{3+} ions are presented in S1 and S2. Spinel phase (maghemite or magnetite) was also obtained in case of annealed S1 or S3 ribbons, respectively. It could be concluded that the initial amorphous allows were completely converted into oxides after their thermal treatment in air as it can be seen from the calculated parameters (Tables 1 and 3). However significant differences in material dispersity and oxidation were obtained.

4 Discussion and conclusions

Thermal treatment of the amorphous $Fe_{67}B_{14}Co_{18}Si$, $Fe_{40}B_{16}Ni_{40}Mo_4$ and $Fe_{78}B_{15}Mo_2Si_5$ alloys above the crystallization temperature results in formation of multiphase crystalline structure and strongly depends on the additive elements (Co, Ni, Mo). It was shown that the annealing in inert (argon) atmosphere differs from annealing in air. It affects the kinetic of crystallization and registered products. Investigation of thermal stability of ribbon metallic

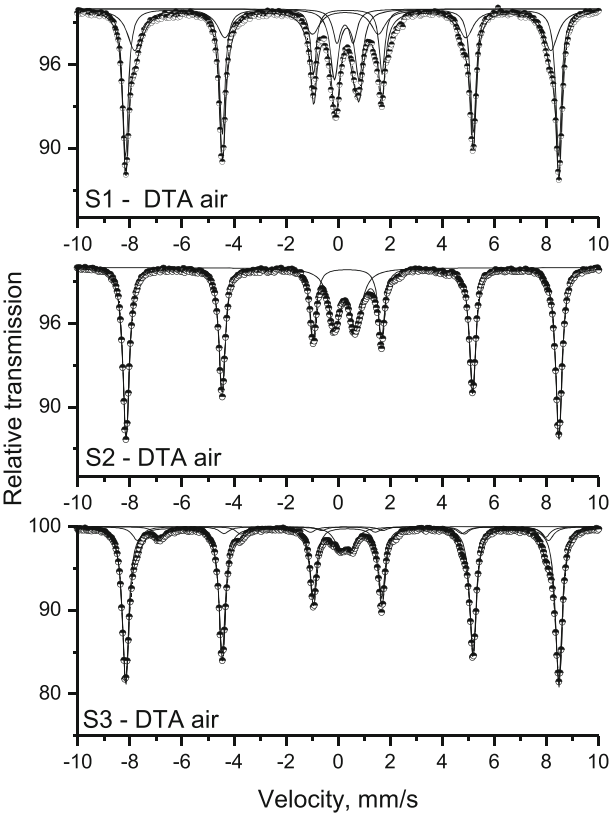

Fig. 8 Mössbauer spectra of thermally treated materials in air: S1 - $Fe_{67}B_{14}Co_{18}Si$; S2 - $Fe_{40}B_{16}Ni_{40}Mo_4$ and S3 - $Fe_{78}B_{15}Mo_2Si_5$

glasses and formation of different intermediate and product compounds is very important for practical application of damaged amorphous alloys, their further reuse and recycling. On the basis of registered transformations by Mössbauer data and thermal analysis, supported by XRD data some conclusions about the dependence of mechanism of the phase transformation of the materials on the chemical composition were made. In order to shed additional light on the processes leading to material damage it is of crucial importance to understand how the microstructure develops during thermal treatment in different atmosphere and, in particular, the rate and extent of phase transformations taking place. These crystallization processes are responsible for the loss of primary advanced magnetic properties and for the operational stability of the studied materials. Mössbauer data clearly show change of iron neighbourhood and rearrangement of additive elements as a result of thermal treatment in inert atmosphere. The end product is composed by intermetallic phase, iron borides and / or silicides. The mostly presented phase is the BCC α-Fe or intermetallic phase and it works as a matrix in which the other phases are embedded [7, 8]. Based on the obtained results further investigation of sustainable reuse of damaged Fe–based amorphous materials will be done. The preliminary results indicate that the homogeneous amorphous structure of studied iron-based metallic glasses is beneficial to azo dye adsorption and degradation.

Acknowledgments The authors gratefully acknowledge the financial support of the Bulgarian National Science Fund at the Ministry of Education and Science - Project № DCOST 01/22/ 2017. This article is based on work from COST Action CA 15102 "Solutions for Critical Raw Materials under Extreme Conditions (CRM-EXTREME)", supported by COST (European Cooperation in Science and Technology).

References

1. Gutfleisch, O., Willard, M.A., Brück, E., Chen, C.H., Sankar, S.G., Liu, J.P.: Magnetic materials and devices for the 21st century: stronger, lighter, and more energy efficient. Adv. Mater. **23**, 821–842 (2011)
2. Liu Y., Sellmyer D.J., Shindo D.: Handbook of advanced magnetic materials. Springer US (2006)
3. Idzikowski, B., Svec, P., Miglierini, M.: Properties and applications of nanocrystalline alloys from amorphous precursors. Series II: Mathematics, Physics and Chemistry, vol. 184, NATO Science Series, Kluwer Academic Publishers (2005)
4. List of critical raw materials for the EU https://ec.europa.eu/growth/sectors/raw-materials/specific-interest/critical_en
5. Online documents, https://ec.europa.eu/easme/en/eu-raw-materials-week-2018-closing-loop-critical-raw-materials
6. Directorate-General for Environment (European Commission): LIFE and the Circular economy, 2017-05-18; https://publications.europa.eu/en/publication-detail/-/publication/ac9eab4b-4045-11e7-a9b0-01aa75ed71a1
7. Grenèche, J.M., Miglierini, M.: Mössbauer spectrometry applied to iron-based nanocrystalline alloys I.: high temperature studies. In: Miglierini, M., Petridis, D. (eds.) Mössbauer Spectroscopy in Materials Science, pp. 243–256. Kluwer Academic Publishers, Dordrecht (1999)
8. Miglierini M., Grenèche JM.: Mössbauer Spectrometry Applied to Iron-Based Nanocrystalline Alloys II. In: Miglierini M., Petridis D. (eds) Mössbauer Spectroscopy in Materials Science. NATO Science Series (3. High Technology), (1999) vol 66. Springer, Dordrecht, pp. 257–272
9. Grenèche JM., Varret F.: Independence of magnetic texture and hyperfine data from Mössbauer spectra of a ferromagnetic metallic glass. Solid State Commun., **54**(11), 985–989 (1985)
10. Prasad, B., Bhatnagar, A., Jagannathan, R.: Amorphous to crystalline transformation of $Fe_{81}B_{13.5}Si_{3.5}C_2$. Appl. Phys. **54**, 2019–2024 (1983)
11. Zhao, L., Li, C., Hao, Z., Liu, X., Liao, X., Zhang, J., Su, K., Li, L., Yu, H., Greneche, J.M., Jin, J., Liu, Z.: Influences of element segregation on the magnetic properties in nanocrystalline Nd-Ce-Fe-B alloys. Materials Characterization **148**, 208–213 (2019)
12. Minić, D.M., Minić, D.M., Žák, T., Roupcová, P., David, B.: Structural transformations of $Fe^{81}B^{13}Si_4C2$ amorphous alloy induced by heating. J. Magn. Magn. Mater. **323**, 400–404 (2011)
13. Sun, X., Cabral-Prieto, A., Yacaman, M.J., Reyes-Gasga, J., Hernandez-Reyes, R., Morales, A., Sun, W.: Nanocrystallization behavior and magnetic properties of amorphous $Fe_{78}Si_9B_{13}$ ribbons Physica B. **291**, 173–179 (2000)
14. Pratar, A., Lilly, T., Rao, S., Patel, K., Chawda, M.: Kinetics of crystallization of a Fe-based multicomponent amorphous alloy. Bull. Mater. Sci. Indian Acad. Sci. **32**, 527–529 (2009)
15. Raja, V., Kishore, S., Ranganathan, S.: Crystallization behaviour of Metglas 2826 MB ($Fe_{40}Ni_{38}Mo_4B_{18}$). Bull. Mater. Sci. Indian Acad. Sci. **9**, 207–217 (1987)
16. Saiseng, S., Winotai, P., Nilpairuch, S., Limsuwan, P., Tang, I.M.: Nanocrystallization in amorphous $Fe_{40}Ni_{40}(Si+B)_{19}Mo_{1-2}$ ribbons. J. Magn. Magn. Mater. **278**, 172–178 (2004)
17. Cornell, R., Schwertmann, U.: The Iron oxides: structure, properties, reactions, occurrences and uses. Weinheim VCH. New York (2006)
18. Gotić, M., Musić, S.: Mössbauer, FT-IR and FE SEM investigation of iron oxides precipitated from $FeSO_4$ solutions. J. Mol. Struct. **834–836**, 445–453 (2007)
19. Niemantsverdriet, J.W., Van der Kraan, A.M., Delgass, W.N., Vannice, M.A.: Small-particle effects in Mössbauer spectra of a carbon-supported iron catalyst. J. Phys. Chem. **89**, 67–72 (1985)

Affiliations

Z. Cherkezova-Zheleva[1] · D. Paneva[1] · V. Petkova[2,3] · J. Krstić[4] · G. Stefanov[5]

[1] Institute of Catalysis, Bulgarian Academy of Sciences, Acad. G. Bonchev St., Bldg. 11, 1113 Sofia, Bulgaria

[2] Department of Natural Sciences, New Bulgarian University, 21 Montevideo Str., 1618 Sofia, Bulgaria

[3] Institute of Mineralogy and Crystallography, Bulgarian Academy of Sciences, bl. 107, Acad. G. Bonchev Str., 1113 Sofia, Bulgaria

[4] Institute of Chemistry, Technology & Metallurgy, Department of Catalysis & Chemical Engineering, University of Belgrade, 12 Njegoseva, Belgrade 11000, Serbia

[5] Institute of Metal Science, equipment, and technologies with Center for Hydro- and Aerodynamics "Acad. A. Balevski", Bulgarian Academy of Sciences, 67 "Shipchenski prohod" St., 1574 Sofia, Bulgaria